Journal of Industrial and Engineering Chemistry 19 (2013) 1153–1161

Contents lists available at SciVerse ScienceDirect

Journal of Industrial and Engineering Chemistry

journal homepage: www.elsevier.com/locate/jiec

Acid modified local clay beads as effective low-cost adsorbent for dynamic adsorption of methylene blue

M. Auta, B.H. Hameed *

School of Chemical Engineering, Engineering Campus, Universiti Sains Malaysia, 14300 Nibong Tebal, Penang, Malaysia

ARTICLE INFO

Article history:
Received 23 May 2012
Accepted 7 December 2012
Available online 17 December 2012

Keywords:
Adsorption
Column study
Thermodynamics
Kinetics
Isotherms
Desorption

ABSTRACT

Locally sourced clay was harnessed to study its adsorptive potential of methylene blue (MB) in wastewater streams. The clay was modified with sulfuric acid and aluminum hydroxide. The raw and modified freeze dried clay bead RHC and MHC were subjected to batch and batch/fixed-bed adsorption studies, respectively. Elemental analysis, morphological structures were determined, and surface area of 19.3 (RHC) and 101.2 (MHC) m^2/g were obtained. Langmuir, Freundlich and Redlich–Peterson isotherms models were analyzed and the modification increased adsorption capacity from 58.02 to 223.19 mg/g at 30 °C. The MB adsorption on RHC/MHC was spontaneous, exothermic and obeyed pseudo-second-order model.

1. Introduction

The existence of clay is synonymous to the age of the planet earth but yet its applicability has not been exhausted. Clays either in natural form or processed has found applications in many facets of life, these includes: construction, farming, catalyst support, in detergent industries, adsorption, chemical industry, beverage, photochemical, ceramics, paper filling and coating, sensors and biosensors [1]. Raw and modified clays have been used extensively for adsorption purposes but the fact that new challenges of pollution problems keeps emanating, it calls for a continuous research towards finding a cheaper, effective and efficient solution to the problems [2,3]. One form of the commonest problems of pollution is indiscriminate discharge of untreated dyes to the environment which affects the entire ecosystem due to their low-degradability, mutagenic and carcinogenic effect on man and constituting as impediment to free penetration of light in water hence affecting photosynthesis ability of aquatic plants [4–6]. Amongst methods of beneficiation of clay for adsorption processes, calcinations, acid treatment, pillaring, cation and anion exchange have yielded good results in producing clay adsorbents [7,8]. Clays are very good substitute for expensive commercial activated carbon used in adsorption processes [9,10]. They have many advantages over other low cost adsorbents such as availability, affordability, ion exchange capability, high adsorption capacity and surface area, mechanical and chemical stability, and different structural and surface characteristics [11].

Nano-meter scale nature of clay which enhances its surface area as well as favorability in adsorption processes is still a major challenge because of difficulties in the dispersing or separation procedures they pose after usage [12,13]. Many adsorption processes using clay adsorbents employ services of other separation techniques such as decantation, filtration and centrifugation for the purpose of separating the adsorbent from the supernatant thereby increasing labor and cost of the adsorption activity; and moreover, the use of these additional techniques in adsorption process are yet to be standardized [14].

Application of adsorption technique for large waste-water treatment usually employs continuous adsorption process while selective sorption and performance of the adsorbent in the process are determined in batch adsorption studies. The advantages of continuous adsorption process over batch process are that large volume of polluted water can be treated at shorter time, high possibility of scale up from laboratory level and the process is much easier to operate [15].

This study is aimed at investigating the potential of abundant local clay from Ipoh in Perak state of Malaysia as substitute to commercial activated carbon adsorbent for adsorption of methylene blue from aqueous solution in a fixed-bed column. The acid treated, cationized and calcined local clay was transformed into beads to reduce labor and time wastage often incurred whenever powdered clay adsorbents are used for adsorption. Desorption test of the modified local clay was investigated.

* Corresponding author. Tel.: +6045996422; fax: +6045941013.
E-mail address: chbassim@eng.usm.my (B.H. Hameed).

1226-086X/$ – see front matter © 2012 The Korean Society of Industrial and Engineering Chemistry. Published by Elsevier B.V. All rights reserved.
http://dx.doi.org/10.1016/j.jiec.2012.12.012

2. Materials and methods

2.1. Materials

A synthetic textile dye, methylene blue (MB), sulphuric acid (H_2SO_4) and aluminum hydroxide ($Al(OH)_3$) of analytical grade were purchased from Sigma–Aldrich chemicals, Merck chemical company and R & M marketing Essex, U.K., respectively; and used without further purification. The clay adsorbent used was gotten from Ipoh in Perak state of Malaysia; it was crushed, ground, sieved to particle sizes of 20–45 μm and dried at 100 °C in an oven for 8 h.

2.2. Preparation of clay adsorbent

The dried local clay (HC) was activated with 2 M H_2SO_4, ratio 0.2 g clay/mL (clay/acid) in a 500 mL beaker placed on hotplate magnetic stirrer; the temperature of the mixture was set at 90 °C and stirred vigorously for 3 h. Then the clay was washed with distilled water to reduce excess moieties and to ensure that the supernatant attain neutrality (pH 6.8–7), thereafter the clay was dried in an oven at 100 °C for 6 h. The dried acid activated HC was refluxed for 2 h at 90 °C after adding about 100 mL of 0.5 M $Al(OH)_3$; the refluxed solution was allowed overnight before washing. The acid activated refluxed clay solution was dried in an oven at 110 °C and then calcined for 3 h at 500 °C. The calcined HC was transformed into beads using sodium alginate binder before freeze drying. Raw dried HC was also molded into beads with the aid of sodium alginate binder and freeze dried. The raw freeze dried HC beads (RHC) and the freeze dried modified HC beads (MHC) both of particle sizes between 1 and 2 mm were kept in air tight container for further use. The RHC and MHC structures are presented in Fig. 1.

2.3. Characterization of the clay adsorbents

The RHC and MHC adsorbents were characterized for elemental analysis, surface morphology and surface area using scanning electron microscope (SEM/EDX analyzer) and Brunauer Emmett Teller (BET) analysis, respectively.

Energy-dispersive X-ray spectroscopy (EDX) for elemental analysis and morphological structure of the adsorbents were performed using scanning electron microscope (Model EMJEOL-JSM6301-F) with an Oxford INCA/ENERGY-350 microanalysis system.

The Brunauer Emmett Teller (BET) analysis was carried out by nitrogen adsorption–desorption method using nitrogen temperature (−196 °C) with an autosorb BET apparatus, Micrometrics ASAP 2020, surface area and porosity analyzer. The analysis procedure was automated and operated with static volumetric techniques. The sample was first degassed at 200 °C for 2 h before each measurement was recorded.

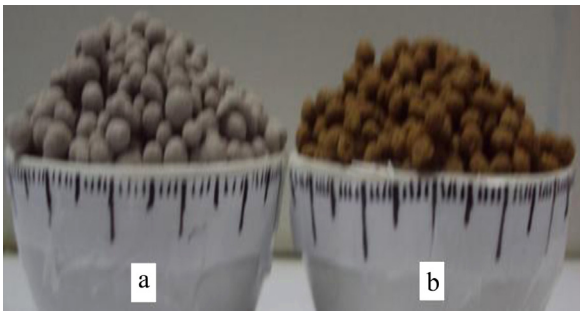

Fig. 1. Structural view of the adsorbents (a) MHC and (b) RHC.

2.4. Batch equilibrium adsorption studies

The batch equilibrium adsorption studies were undertaken using a set of Erlenmeyer flasks (250 mL) containing 200 mL of MB solutions at various initial concentration (30–300 mg/L). The RHC adsorbent 0.2 g (1–2 mm) was added and placed in water bath isothermal shaker at 30 °C for 12 h, at 140 rpm shaker speed to attain equilibrium. The final concentrations of MB solution in the flasks after equilibrium were determined using UV–vis spectrophotometer (Shimadzu UV/Vis 1601 spectrophotometer, Japan) at maximum wavelength of 668 for MB. Afterwards, temperature of water bath shaker was adjusted to 40 °C and 50 °C, and the procedure was repeated with another set of flasks containing similar different initial MB concentration. The adsorbent was changed to MHC and similar procedure was administered. The amount of the MB adsorbed at time t, at equilibrium Q_e (mg/g) was evaluated by the following equation:

$$Q_e = \frac{C_o - C_e}{W} \quad (1)$$

where C_o and C_e (mg/L) are the liquid-phase concentration of the MB at initial and at equilibrium, respectively; $V(L)$ is the volume of the solution; and $W(g)$ is the mass of the dried adsorbent (RHC or MHC).

2.5. Effect of solution pH on MB adsorption by both RHC and MHC

The effect of initial pH on MB adsorption on both RHC and MHC was carried out using either 0.1 M NaOH or 0.1 M HCl for adjustment of pH of the solutions in the range 3–12. Adjustment of the pH was valued using pH meter (Model Delta 320, Mettler Toledo, China). The study was administered in a set of 250 mL Erlenmeyer flasks charged with 200 mg/L and 0.20 g of the MB concentration and adsorbent beads, respectively at a temperature of 30 °C for 12 h.

2.6. Batch kinetic studies

A limiting step upon which adsorption process design is based is the transfer rate of solute to the adsorbent from the bulk solution. This was done by determining the MB solution concentration at pre-set intervals of time. The measure of the dye at time t adsorbed, Q_t (mg/g) was calculated using equation:

$$Q_t = \frac{(C_o - C_t)V}{W} \quad (2)$$

where C_o and C_t (mg/L) are the liquid-phase concentration of the MB at the initial and any time t, respectively; $V(L)$ is the volume of the solution; and $W(g)$ is the mass of the either RHC or MHC adsorbent used.

2.7. Desorption studies

An amiable quality of an adsorbent is its predisposition for reuse. This was investigated through desorption and regeneration studies which are valuable attributes in adsorption processes. The recovered pre-adsorbed 0.2 g of MHC from 100 mg/L dye solution was slightly washed using distilled water to eliminate the un-adsorbed MB on the sorbent surface, air dried and then placed in 100 mL of distilled water of pH 4 in a water-bath shaker at 30 °C, shaker speed of 140 rpm for the predetermined equilibrium time of the adsorption process. Desorption efficiency of MB was determined as:

$$\text{Desorption efficiency}\,(\%) = \frac{M_d V_d}{W \times Q_e 100} \times 100 \quad (3)$$

where M_d (mg/L) is the concentration of MB desorbed from pre-adsorbed MHC adsorbent, V_d (mL) is the volume of the solution used for desorption, W (g) is the mass of the pre-adsorbed adsorbent, Q_e (mg/g) is the amount of the pre-adsorbed adsorbate on the adsorbent. The procedure was repeated until there was significant difference in desorption efficiency.

2.8. Fixed-bed column experiment

A 19.5 cm length with inner diameter of 1.2 cm Pyrex glass tube was used as the fixed-bed column. The graduated column had a stainless steel sieve at the bottom on which a layer of glass beads were placed. Influent concentration, bed depth and flow rate effects on the adsorption process were studied. A known quantity 1.2, 2.0 and 3.2 g of MHC was measured into the column to give the desired 2.5, 3.6 and 4.5 cm bed height, respectively. To avoid non-uniform flow (axial dispersion) of the solution and fluidization, some quantity of glass beads of same sizes were placed in the column. A 50, 100 and 200 mg/L initial MB concentration was introduced at flow rates of 5, 8 and 10 mL/min, the solution was pumped upward with the aid of a peristaltic pump (Master-flex, Cole-Parmer Instrument Co.). The adsorption experiments were carried out at 30 °C and the influent concentrations and concentrations at interval of times of MB were measured using UV–vis spectrophotometer (Shimadzu UV/Vis 1700, Japan) at maximum wavelength, λ_{max} = 668 of MB.

2.8.1. Analysis of column data

The sorption behavior of MB by MHC in the column was depicted in the mass transfer zone of the breakthrough curves. As the solution initially came in contact with the fresh porous adsorbent, high removal of MB was noticed which gradually changed with time until breakthrough profile was established. The breakthrough curves were obtained by plotting C_t or C_t/C_o (mg/L) against V_t (mL) or t (min); where C_t is the effluent concentration, C_o influent concentration, V_t is treated volume and t is the service time. The treated effluent volume, V_t was determined as:

$$V_t = Qt_e \tag{4}$$

where Q is the volumetric flow rate (mL/min) and t_e is the time at exhaustion (min).

The maximum column capacity (q_{total} (mg)), for a given concentration of feed and flow rate is a measure of the area under the plot of the concentration of MB adsorbed. This can be expressed as, $C_{ad}(C_{ad} = C_o - C_t)$ mg/L, against effluent time t (min) and is obtained from Eq. (5) [16]:

$$q_{total} = \frac{Q_A}{1000} = \frac{Q}{1000}\int_{t=0}^{t=t_{total}} C_{ad}\,dt \tag{5}$$

where t_{total}, Q and A are the total flow time (min), volumetric flow rate (mL/min) and the area under the breakthrough curve, respectively. Equilibrium uptake ($q_{eq(exp)}$) (mg/g) is calculated as:

$$q_{eq(exp)} = \frac{q_{total}}{m} \tag{6}$$

where m is the total amount of adsorbent (g) in the column. The total amount of dye sent to the column (W_{total}) is calculated from this equation:

$$W_{total} = \frac{C_o Q t_{total}}{1000} \tag{7}$$

The total amount of dye in percentage removed is the quotient of the maximum capacity of the column (q_{total}) divide by the total amount of dye sent to the column (W_{total}) expressed as:

$$R = \frac{q_{total}}{W_{total}} \times 100 \tag{8}$$

3. Results and discussion

3.1. Characterization of RHC and MHC

The N_2 adsorption/desorption isotherms at 77 K for RHC and MHC are shown in Fig. 2. The BET surface area for RHC and MHC were 19.32 and 101 m^2/g; cumulative pore volume of 0.1095 and 0.2492 cm^3/g; and, average pore diameter of 2.2 and 9.8 nm, respectively. The isotherms of Fig. 2 exhibited behaviors of both Type II and IV isotherms which denotes non-porous and mesoporous adsorbents according to the IUPAC classification [17].

The EDX carried out on RHC and MHC using the scanning electron microscope are presented in Fig. 3. The EDX spectrum for elemental analysis in RHC showed a high presence of exchangeable cations which were virtually absent in the MHC spectrum; the RHC had 0.17 wt% of Mg and 1.03 wt% of Ca while MHC had none, and there was variation of elements between the two adsorbents. This could be attributed to acid treatment and cation exchange with aluminum hydroxide of the HC clay that were carried out. Similar observation was made when some cations such as Na^+, K^+, and Ca^{2+} leached out during acid treatment of montmorillonite clay [18,19]. The morphological structure showed agglomerated and approximately equal sizes of particles in the RHC micrograph as compared with the scattered uneven clay particles of the MHC micrograph. This could be attributed to concurrent substitution of trivalent ions with divalent ions (Ca^{2+}, Fe^{2+}, Mg^{2+} for Al^{3+}) in the octahedral layers and tetravalent ions with trivalent ions ($A1^{3+}$ for Si^{4+}) in the tetrahedral layers; loss of some cations during acid treatment; and, loss of some volatile organic substances during calcinations which all occurred during the surface area developmental modification that the raw HC was subjected to. This observation is similar to report in literature of morphological structures of raw, pillared and calcined montmorillonite clays in a study of reactive adsorption of methylene blue on montmorillonite via an ESI-MS [20].

3.2. Effect of solution pH on MB adsorption

The measure of the acidity or basicity (pH) of the dye solution was carried out to enhance comprehensive evaluation of the adsorption process as pH is an invaluable integral part of aqueous solution studies [21]. The MB adsorption on both RHC and MHC was done within the range of pH 3–12. A careful observation revealed that higher adsorption of MB was realized at higher

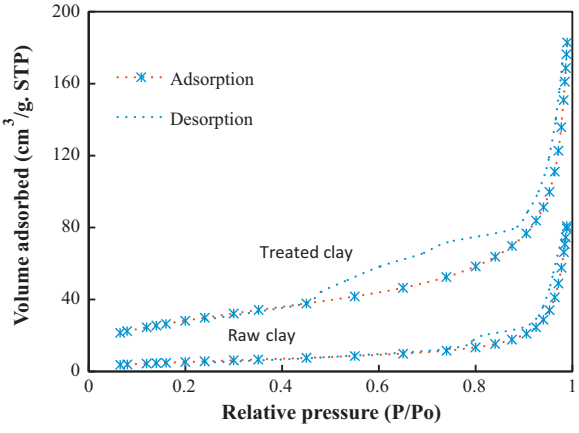

Fig. 2. The BET analysis of RHC and MHC.

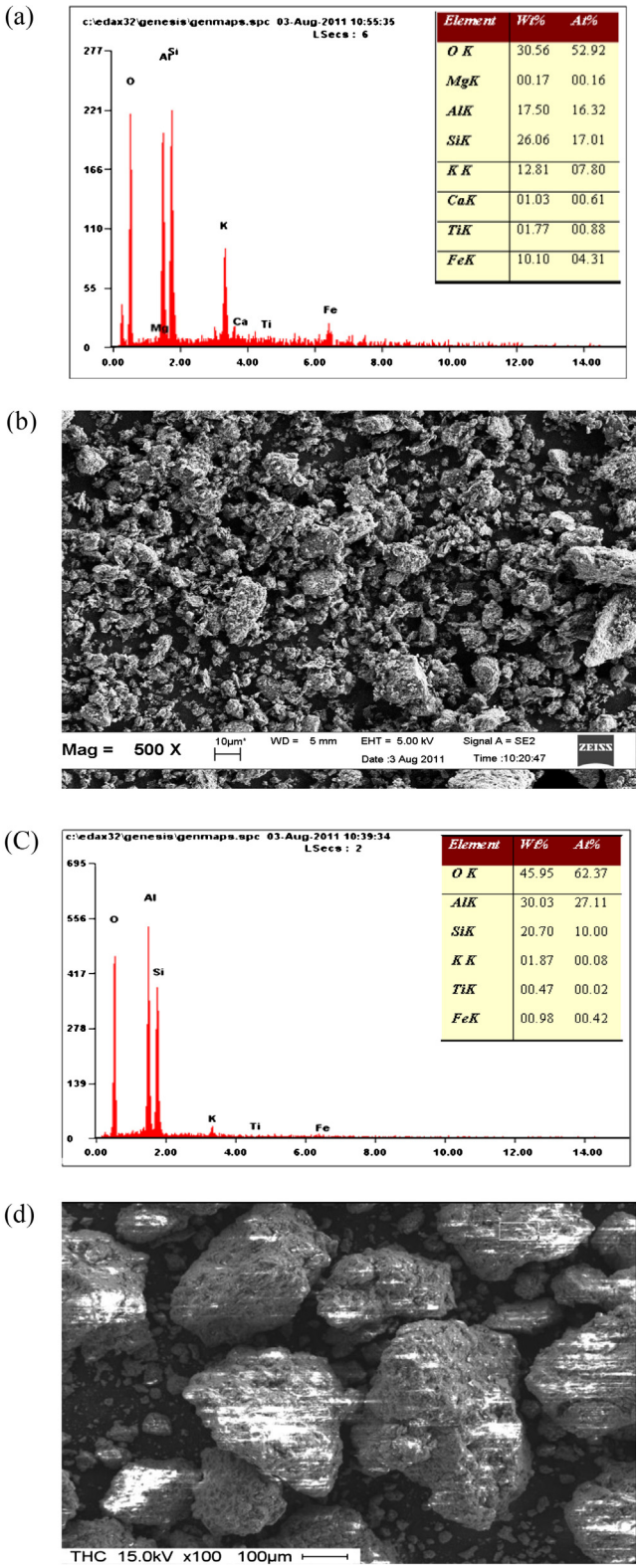

Fig. 3. EDX analysis: (a) RHC spectrum, (b) RHC micrograph, (c) MHC spectrum, (d) MHC micrograph.

solution pH that is when the hydroxide ion concentration was greater than the hydrogen ion concentration. This was attributed to the electrostatic attraction due to coulombic forces between the positive MB molecules and the negatively charged active sites on the adsorbents surfaces. At lower pH 3–4 where protonation of H^+ activities dominated and influencing the adsorbent surfaces to become positively charged, repulsion reaction between the MB molecules and the adsorbent active surfaces resulted. These repulsive activities lead to poor adsorption of MB on both RHC and MHC at lower pH ranges. A percentage increase of 462.50 and 72.73% was observed for MB adsorption by RHC and MHC, respectively when the initial solution pH was changed from 3 to 12. Similarly, MB adsorption on an adsorbent increased from 312 to 580 mg/g when the solution pH was changed from 4 to 11 [22]. Adsorption of MB on both adsorbents showed increase with elevation of pH until a point (>pH 10) where further increase did not have significant impact, this is comparable to MB highest adsorption results obtained at similar higher pH values pattern [22–24]. The effect of solution pH on the adsorption of MB on both RHC and MHC is shown in Fig. 4.

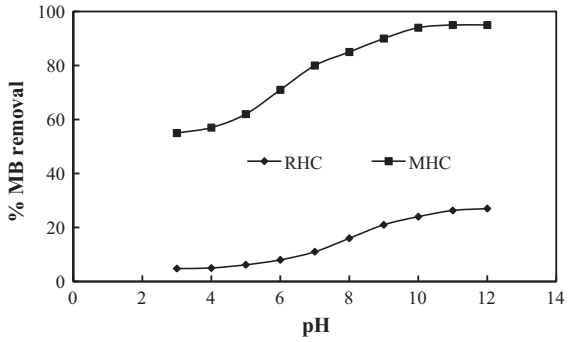

Fig. 4. Effect of solution pH 3–12 of MB adsorption on both RHC and MHC at 30 °C.

3.3. Effect of initial dye concentration on adsorption

The adsorption of MB by either RHC or MHC adsorbent was found to propagate with subsequent increase in the initial dye concentration of the influent. This was due to increase in the mass transfer to the vacant pore sites of the adsorbent. The reverse was the case in terms of the percentage removal at various initial concentrations of the dye solutions. At lower concentration of the dye solution, a greater percentage removal was prominent than at higher concentrations. It was attributed to probable proportionate number of vacant sites to the molecules of the adsorbate at those lower concentrations; this may have contributed also to the fast uptake of dye at the initial stages of the adsorption process which were determined with the aid of the UV–vis spectrophotometer. Similar trend was reported in the adsorption of MB on commercial activated [25], and for removal of Reactive Blue 19 by modified bentonite [26]. The maximum capacity of the adsorbent was determined when the dye and adsorbents were at equilibrium position. The graphs in Fig. 5 showed that, dynamic equilibrium position was attained faster at lower concentration of the MB than at higher concentrations.

3.4. Adsorption isotherm

At position of dynamic equilibrium of adsorption process, there arise a need to determine the adsorbate spreading between the liquid phase and solid phase; this information can be obtained through adsorption isotherms studies [4]. Isotherms behavior of the MB adsorption on both RHC and MHC adsorbents were studied using Langmuir, Freundlich and Redlich–Peterson models.

The non-linear form of the Langmuir isotherm model [27] is given as:

$$Q_e = \frac{Q_m C_e b}{1 + bC_e} \quad (9)$$

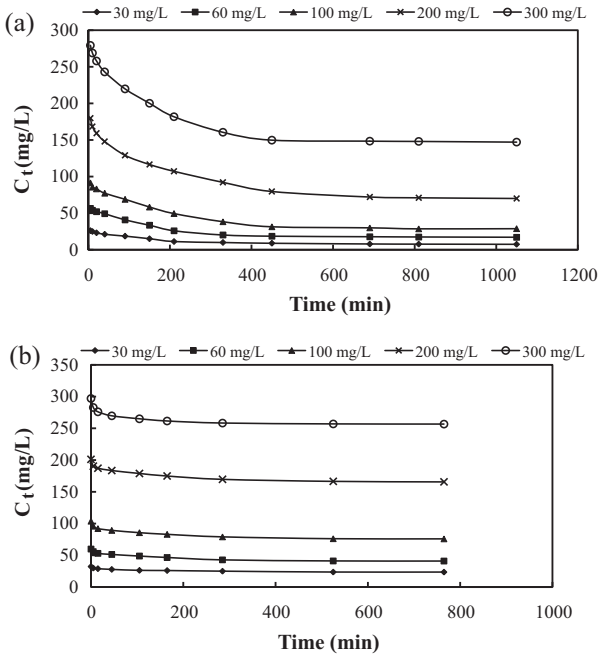

Fig. 5. MB adsorption at different initial concentrations and contact time at 30 °C (a) RHC and (b) MHC.

where C_e (mg/L), is the equilibrium concentration of MB adsorbed; Q_e (mg/g), is the amount of MB adsorbed; Q_m and b (Langmuir constants), the monolayer adsorption capacity and affinity of adsorbent towards adsorbate, respectively. Langmuir constants generated from sorption data plot of Q_e against C_e for both RHC and MHC shown in Fig. 6 are summarized in Table 1.

The Freundlich isotherm is based on the premise that adsorption occurs on rare heterogeneous surfaces sites with different energy of adsorption and are also non-identical. The non-linear form of the Freundlich isotherm was used to investigate the adsorption process adherence to the model, the equation [28] is given as:

$$Q_e = K_F C_e^{1/n} \tag{10}$$

where Q_e (mg/g) is the amount of dye adsorbed at equilibrium; C_e (mg/L) is the equilibrium concentration of the adsorbate; K_F ((mg/g) (L/mg)$^{1/n}$ and n (dimensionless) are the Freundlich equilibrium coefficients. The value of 'n' a heterogeneous factor, gives information on favorability of adsorption process; while $1/n$ relays information on adsorption intensity and, K_F is the adsorption capacity of the adsorbate. The values of the model parameters obtained from the plot of Q_e against C_e shown in Fig. 6 are presented in Table 1.

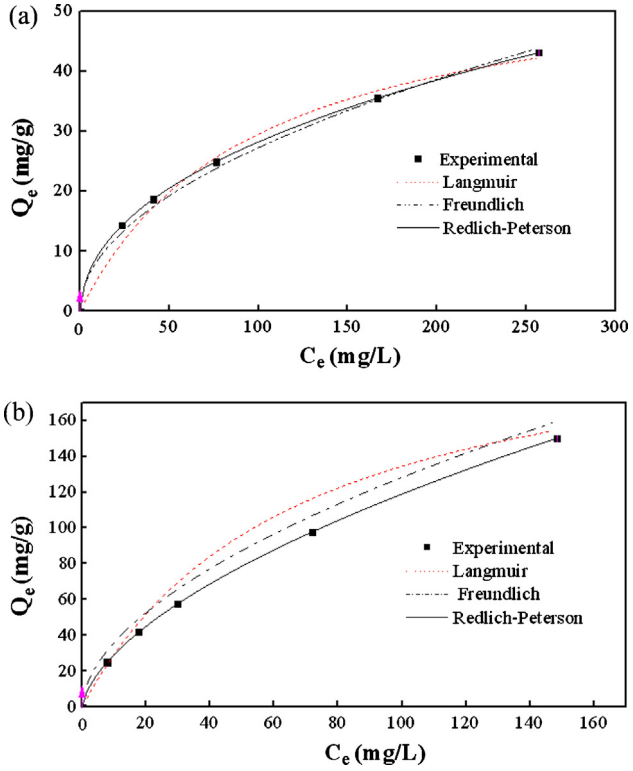

Fig. 6. Langmuir, Freundlich and Redlich–Peterson isotherms plot of (a) RHC and (b) MHC at 30 °C.

The Redlich–Peterson isotherm model [29] contains three parameters and it involves features of both Langmuir and Freundlich isotherms. The equation is as follows:

$$Q_e = \frac{AC_e}{1 + BC_e^r} \tag{11}$$

Taking the natural logarithm gives the following equation:

$$\ln\left(A\frac{C_e}{Q_e} - 1\right) = g\ln(C_e) + \ln(B) \tag{12}$$

Since three parameters Redlich–Peterson isotherm linear model analysis is impossible, a trial and error optimization technique was used to evaluate the three model's constants A (L/g), B (L/mg)^g and g from the pseudo-linear plot expressed as Eq. (12). A general trial and error procedure which is applicable to computer operations to determine the coefficient of determination, R^2 for series of values of A for the linear regression of $\ln(C_e)$ on $\ln[A(C_e/Q_e) - 1]$ and to obtain the best value of A which yields a maximum optimized value of R^2 was used [30].

Table 1
Langmuir, Freundlich and Redlich–Peterson model isotherms parameters for MB.

Isotherms	Parameters	RHC			MHC		
		30 °C	40 °C	50 °C	30 °C	40 °C	50 °C
Langmuir	Q_m (mg/g)	58.02	54.09	47.37	223.19	219.88	216.95
	b (L/mg)	0.0104	0.0047	0.0095	0.0086	0.0271	0.0704
	R^2	0.949	0.980	0.974	0.977	0.948	0.907
Freundlich	K_F ((mg/g) (L/mg)$^{1/n}$	2.68	0.80	2.25	10.08	11.10	8.49
	$1/n$	0.5036	0.6536	0.5049	0.691	0.602	0.508
	R^2	0.931	0.929	0.911	0.932	0.941	0.954
Redlich–Peterson	g	0.574	0.582	0.387	0.4339	0.4873	0.4784
	B (L/mg)^g	1.330	5.646	10.1474	2.1472	1.420	1.8081
	A (L/g)	5.560	20.676	10.310	20.017	17.797	18.7668
	R^2	0.979	0.971	0.998	0.974	0.978	0.982

Table 2
Comparison of monolayer adsorption of MB onto various adsorbents.

Adsorbent	Adsorption capacity (mg/g)	Reference
RHC	58.02	This work
MHC	223.19	This work
Natural palygorskite clay	48.39	[23]
Heat-treated palygorskite clay	78.11	[23]
Montmorillonite clay	289.12	[24]
Persian Kaolin	29.85	[32]
NaOH-treated pure kaolin	20.49	[33]
NaOH-treated raw kaolin	16.34	[33]
Bentonite	173	[34]

The three isotherms under study all described the adsorption of MB on both RHC and MHC but not without some level of variance of their fitness. The best fit of isotherm was selected based on the highest correlation coefficient (R^2) value (closest to unity) which described the fitness of the isotherm to the experimental data. Similar evaluation was reported during analysis of isotherms for adsorption of methylene blue on walnut shell activated carbon [31].

Redlich–Peterson isotherm model had the best fit than the other two parameters models for the adsorption of MB on both RHC and MHC (Figures not shown); this was evident in the R^2 values presented in Table 1. The values of g obtained were far from unity depicting tendencies of approaching Freundlich and not Langmuir isotherm which is approached when $g = 1$. However, the three isotherms fitness to the adsorption of MB by both RHC and MHC revealed that Langmuir and Freundlich isotherms came second and third respectively after Redlich–Peterson. The Freundlich and Redlich–Peterson isotherm model involves surface heterogeneity of the MB adsorption process while the homogeneous behavior of MB adsorption process was informed by Langmuir isotherm model. Similar result to MB adsorption as obtained from this study was reported for study on adsorption of MB onto activated carbon produced from steam activated bituminous coal where from their correlation coefficient values R^2, the adsorption equilibrium modeling studies were described best by Redlich–Peterson and then followed by Langmuir and Freundlich isotherm models, respectively [22]. Also, in regression analysis for the sorption isotherms of basic dyes on sugarcane dust studies, one of the results obtained was similar to the ones obtained in this study [30]. Although Freundlich isotherm was the least fitted model, favorable adsorption of MB on the heterogenous surfaces of both RHC and MHC was observed; this is going by the values of $n > 1$ and $0 < 1/n < 1$ which were obtained as shown in Table 1, satisfying favorable and heterogenous conditions, respectively of the model. A good fit of Langmuir model showed that there was monolayer coverage of MB on the adsorbent surfaces. The monolayer coverage obtained from this work can be compared with similar published data as shown in Table 2.

3.5. Adsorption kinetic models

Non-linear pseudo-first order equation [35] is given as:

$$Q_t = Q_e(1 - e^{-k_1 t}) \quad (13)$$

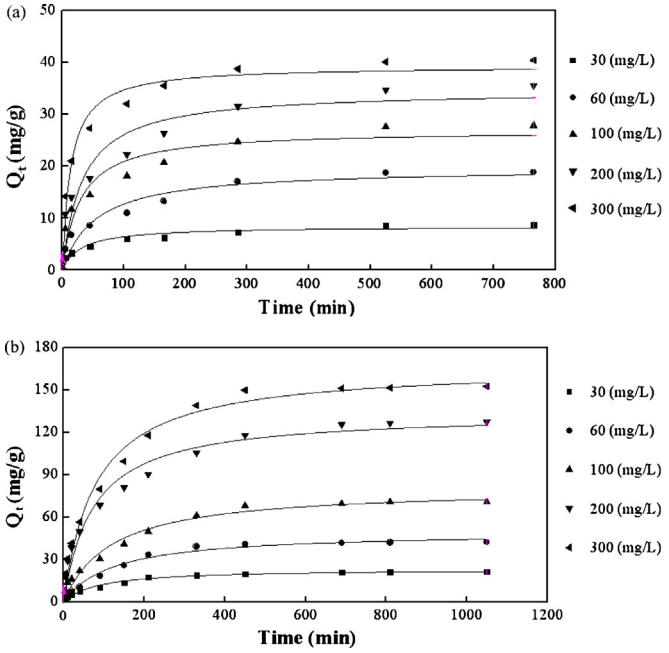

Fig. 7. Pseudo-second-order kinetics plot for adsorption of MB on (a) RHC and (b) MHC at 30 °C.

where Q_e and Q_t (mg/g), are the amount of MB adsorbed on MHC at equilibrium and at time t (h) respectively; k_1 (h^{-1}), is the rate constant of adsorption. Parameters of the rate equation for the two adsorbents are presented in Table 3; these were obtained from plots of Q_t against t (Figures not shown) for various temperature studied.

The pseudo-second order adsorption model [36] equation is given as:

$$Q_t = \frac{k_2 Q_e^2 t}{1 + k_2 Q_e t} \quad (14)$$

where k_2 (g/mgh) is the rate constant of second order adsorption. Plots of Q_t versus t at 30 °C for various concentrations studied gave very good curves as shown in Fig. 7. The pseudo-second-order parameters for adsorption of MB by MHC generated from the plots are presented in Table 3.

Adsorption kinetic studies gave information on the rate of MB uptake by the MHC adsorbents which also helped in controlling equilibrium time of the process. This type of information is indispensable for designing and modeling, and for selection of optimum operating conditions for large scale (column) set up of adsorption process. Results of the two kinetic models tested showed that the adsorption of MB on the MHC adsorbent was described well by pseudo-second-order model as compared with pseudo-first-order kinetic model. This means that the adsorption mechanism was the rate controlling step which is in accordance with the equation establishing the model. The pointer to pseudo-second-order was evident from the high values of

Table 3
Pseudo-first and Pseudo-second-order reaction parameters for MB adsorption on MHC at 30 °C.

Dye conc. (mg/L)	Q_{exp} (mg/g)	Pseudo-first-order parameters			Pseudo-second-order parameters		
		k_1 (h^{-1})	Q_{cal}	R^2	k_2 (g/mgh) 10^4	Q_{cal}	R^2
30	20.822	0.0087	20.622	0.973	4.96	23.277	0.985
60	41.601	0.0069	42.419	0.994	1.63	49.629	0.988
100	69.397	0.0067	69.982	0.970	1.05	80.632	0.979
200	125.341	0.0092	120.338	0.936	1.02	133.520	0.973
300	150.065	0.0089	149.137	0.967	0.751	166.763	0.983

correlation coefficient R^2 compared with those of pseudo-first-order kinetics. In a similar manner, pseudo-second-order kinetic model described the adsorption kinetics of Methyl Orange (MO), Orange G (OG) and Brilliant Red X-3B (X-3B), from their aqueous solutions with mesoporous silica SBA-3 as an adsorbent [37].

3.6. Intra-particle diffusion model

Adsorption involves motion of molecules from the bulk aqueous solution to the adsorbent surface across the boundary layer, and diffusion of the molecules into adsorbent pores. The MB adsorption on MHC was studied to determine whether the process was controlled by either boundary layer diffusion or intra-particle diffusion model or both. The Weber and Morris (Intra-particle diffusion) model equation [38] used is expressed as follows:

$$q_t = k_{id} t^{1/2} + C \quad (15)$$

where q_t (mg/g) is the amount of MB adsorbed at time t, and k_{id} (mg/g min$^{1/2}$) is the rate constant for intra-particle diffusion. The nature of plots of q_t against $t^{1/2}$ which were multi-linear signified that the adsorption process was controlled by two or more steps [39]. The rate constants and boundary layer thickness C, were obtained from the slope and intercept, respectively of the linear plots (Figure not shown) for both the boundary layer diffusion (early stage of the adsorption process-curved portion of the plot) and intra-particle diffusion sections (later part of adsorption-linear portion of the plots). The result as shown in Table 4 showed that the constant C was found to increase from 17.21 to 144.80 with increase in initial MB concentration from 30 to 300 mg/L at intra-particle diffusion region while at the boundary layer section, the constant C increased from 0.535 to 12.53 with similar corresponding initial MB concentration increase. This depicted chances of increased internal mass transfer process as against external mass transfer which decreases as the boundary layer thickness increases [40]. The intra-particle diffusion rate constant k_{i2} were lower than that of boundary layer diffusion k_{i1}, signifying that intra-particle diffusion controlled the MB adsorption on MHC. Intra-particle diffusion rate controlling was further predicted going by its correlation coefficient R^2 values closeness to unity than those of boundary layer diffusion.

3.7. Adsorption thermodynamics

Thermodynamic studies for adsorption of MB on MHC at various temperatures of 30, 40 and 50 °C were carried out. This was done to determine the spontaneity of the adsorption process. The equation used is expressed as:

$$\Delta G = -RT \ln K_0 \quad (16)$$

where R is the universal gas constant (8.314 J/Kmol); T, the absolute temperature (K); K_0 is the distribution coefficient expressed as $K_0 = Q_e/C_e$; and ΔG is the Gibbs free energy.

Van't Hoff equation was used to determine the average standard enthalpy change, the equation is expressed as:

$$\ln K_0 = \frac{-\Delta G}{RT} = \frac{\Delta S}{R} - \frac{\Delta H}{RT} \quad (17)$$

A plot of $\ln K_0$ against $1/T$ gives a graph (Figure not shown) where we can obtain entropy ΔS, from the intercept and enthalpy ΔH, from the slope; which are parameters that provides information on movement of solute (MB) from the bulk to the adsorbent (MHC) surface. Summary of the thermodynamic parameters obtained are summarized in Table 5.

The thermodynamic studies results revealed that MB adsorption on MHC was spontaneous and the degree of dispersion of the process increased proportionally with temperature of the process. This was seen in the negative values (−2.449, −3.549, −4.580 kJ/mol for 303, 313 and 323 K, respectively) of the Gibbs free energy (ΔG) and positive value (0.109 kJ/mol) of entropy (ΔS); this is in agreement with report on thermodynamics properties of Reactive dye adsorption on chitosan adsorbents [41]. Exothermic reaction mechanism described the uptake of MB by MHC as the increase in temperature did not lead to further increase in adsorption and the enthalpy (ΔH) value (−30.487 kJ/mol) evaluated was negative. The magnitude of Gibbs free energy (ΔG) helps in classifying adsorption processes into physical and chemisorptions. Absolute values of ΔG between −20 and 0 kJ/mol connotes physical adsorption while, ΔG values from −80 to −400 kJ/mol speaks about chemisorptions [42,43] Adsorption of MB on MHC were physical in nature, this is in accordance with ΔG shown in Table 5. Adsorption of Acid Blue 25 dye on waste tea activated carbon was reported to be physical in nature; this is similar to the result obtained in this study [44].

3.8. Desorption studies

One of the extremely essential ways to economically assess a good adsorbent is its reusability qualities [45]. The reusability or desorption test of MB adsorbate release from the pre-adsorbed

Table 4
Intra-particle diffusion model parameters of MB adsorption on MHC at 30 °C.

Dye concentration (mg/L)	Boundary layer diffusion			Intra-particle diffusion		
	k_{i1} (mg/(g min$^{1/2}$))	C	R^2	k_{i2} (mg/(g min$^{1/2}$))	C	R^2
30	1.063	0.535	0.919	0.133	17.21	0.985
60	2.369	1.436	0.986	0.131	38.13	0.991
100	3.266	3.092	0.841	0.252	62.80	0.995
200	5.368	7.316	0.853	0.234	100.80	0.983
300	7.451	12.530	0.995	0.863	144.80	0.996

Table 5
Fixed-bed column data parameters obtained at different influent concentration (50–200 mg/L), bed depth (2.5–4.5 cm) and flow rates (5–10 mL/min).

Influent concentration (mg/L)	MHC bed depth, H (cm)	Flow rate, Q (mL/min)	q_{total} (mg)	q_e (mg/g)
50	2.5	5	32.689	27.241
50	4.5	5	127.460	39.858
50	3.6	5	58.086	29.043
100	3.6	5	117.949	58.975
200	3.6	5	153.425	76.712
100	3.6	8	151.428	75.714
100	3.6	10	75.911	37.956

MHC was carried out at initial dye solution pH 4 as a result of poor adsorption of the dye on the adsorbent at lower pH observed during effect of pH studies. At that aqueous solution condition, the MHC surface became more positively charged which promoted electrostatic repulsion between the MHC surface and cationic MB adsorbate. These activities enhanced population of the adsorbate molecules from MHC into the desorbing solution. After three repeated desorption tests, the following results from the first to the third runs were obtained 61.71, 56.68 and 33.49%, respectively. Electrostatic repulsion desorption analysis has been carried out during adsorption of textile dyes from pine cone adsorbent [46].

3.9. Fixed-bed column studies

Fixed-bed adsorption involves mass transfer between two phases, the solute from the liquid phase to the solid phase adsorbent. Effect of influent concentration, solution flow rate and bed depth on the distribution of MB molecules between the solution and the MHC adsorbent were studied.

3.9.1. Effect of initial MB concentration on fixed-bed column adsorption study

The effect of initial influent concentration of 50, 100 and 200 mg/L at fixed flow rate of 5 mL/min and bed height of 3.6 cm were investigated on breakthrough curve of the fixed-bed column adsorption of MB by MHC. Extended breakthrough time was observed at 50 mg/L lower concentration signifying that more volume of the polluted water was treated. At lower influent concentration which translated to lower mass transfer coefficient, longer time was required for the available active sites of the MHC to be fully saturated. On the contrary, shorter time (<4 h) of breakthrough point attainment with steeper slopes and smaller volume of treated waste-water were the characteristics inherent with higher concentration of 200 mg/L influent solution. The high diffusion coefficient due to higher influent concentration resulted to high demand of the available active sites of MHC by the numerous solute molecules in solution. These results were in agreement with findings in literature [15,47]. The breakthrough curves for initial influent concentration effect on the fixed-bed column study are shown in Fig. 8. The experimental result followed the expected trend of increase in adsorption capacity as the influent concentration increased. The adsorption capacity of 29.04, 58.98 and 76.71 mg/g were obtained with corresponding influent concentrations of 50, 100 and 200 mg/L, respectively. This can be seen in Table 5.

3.9.2. Effect of solution flow rate on fixed-bed column adsorption study

The breakthrough curves for the effect of solution flow rate on the adsorption process are shown in Fig. 9. At fixed 100 mg/L influent concentration and bed depth of 3.6 cm, flow rates of 5, 8 and 10 mL/min were varied. Breakthrough points were observed to occur faster at higher flow rates which were attributed to increased mass transfer. It was expected that as the mass transfer increased at higher flow rates, the adsorption of MB on MHC also should correspondingly increased; this was followed when flow rate changed from 5 to 8 mL/min. At higher flow rate of 10 mL/min, the trend was not followed due to insufficient residence time of the solute in adsorption zone of the column. Therefore, instead of increase in adsorption of MB on MHC, the reverse was the order. This can be seen as summarized in Table 5. Similar results as obtained in this study have been reported [48].

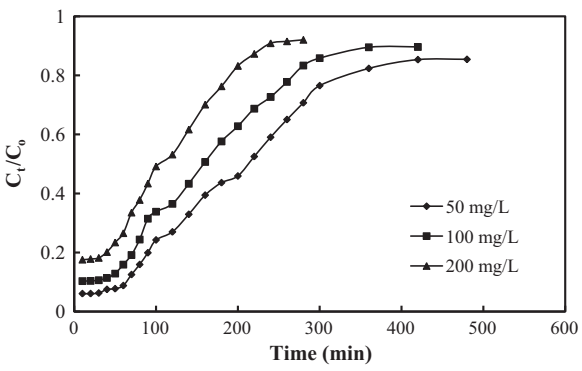

Fig. 8. Breakthrough curves for MB adsorption at different influent concentrations (bed depth = 3.6 cm, flow rate = 5 mL/min, temperature = 30 °C).

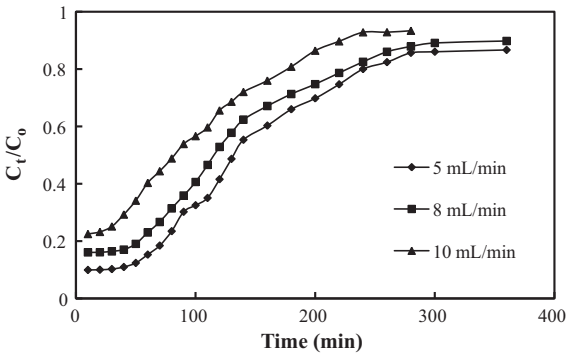

Fig. 9. Breakthrough curves for MB adsorption at different flow rates (influent concentration = 100 mg/L, bed depth = 3.6 cm, temperature = 30 °C).

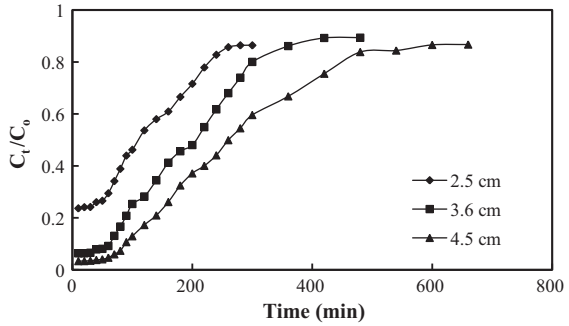

Fig. 10. Breakthrough curves for MB adsorption at different bed depths (influent concentration = 50 mg/L, flow rate = 5 mL/min, temperature = 30 °C).

3.9.3. Effect of MHC bed depth on fixed-bed column adsorption study

MHC bed depths of 2.5, 3.6 and 4.5 cm at fixed influent concentration of 50 mg/L and 5 mL/min flow rate were used to study their effect on MB fixed-bed column adsorption by MHC. The breakthrough curves obtained are shown in Fig. 10. Higher bed depth signifies larger service area for adsorption or increased in active adsorbent sites and increase in contact time between the solute and adsorbent surface [49]. Higher adsorption of MB on MHC was observed at higher bed depths than at lower bed depth in this study as can be seen in Table 5. Breakthrough points were attained faster at shorter bed depths a condition which is prone to axial dispersion phenomenon controlling than the expected solute diffusion trend [50]. Larger volume of the synthetic waste-water was treated in higher bed depth since longer exhaustion time of the bed was also observed.

4. Conclusion

The MHC was a better adsorbent than RHC for removal of MB from synthetic textile waste-waters. The modification of the clay

increased the surface from 19 to 101 m^2/g, pore volume from 0.1095 to 0.2495 cm^3/g and the adsorption capacity from 58.02 to 223.19 mg/g. The isotherm parameters obtained from models revealed that, Redlich–Peterson was the best isotherm that described the adsorption process and then followed by Langmuir and Freundlich isotherms, respectively; for both RHC and MHC. The MB on MHC adsorption process which followed pseudo-second-order kinetics was exothermic, spontaneous and physical; according to results of thermodynamics studies. Reusability test revealed that the MHC can be used a couple of times before disposal.

Acknowledgements

Authors acknowledge the financial support provided by Universiti Sains Malaysia under the Research University (RU) Scheme (Project No. 1001/PJKIMIA/814072) and RU-PRGS grant scheme (Project No. 1001/PJKIMIA/8045026).

References

[1] M. Castellano, A. Turtorro, P. Riani, T. Montanari, E. Finocchio, G. Ramis, G. Busca, Applied Clay Science 48 (2010) 446.
[2] V. Vimonses, B. Jin, C.W.K. Chow, C. Saint, Chemical Engineering Journal 158 (2010) 535.
[3] M. Auta, B.H. Hameed, Chemical Engineering Journal 175 (2011) 233.
[4] M. Berrios, M.A. Martín, A. Martín, Journal of Industrial and Engineering Chemistry 18 (2012) 780.
[5] G. Moussavi, R. Khosravi, Chemical Engineering Research and Design 89 (2011) 2182.
[6] M. Karatas, Y.A. Argun, M.E. Argun, Journal of Industrial and Engineering Chemistry 18 (2012) 1058.
[7] B. Cheknane, O. Bouras, M. Baudu, J.P. Basly, A. Cherguielaine, Chemical Engineering Journal 158 (2010) 528.
[8] G. Rytwo, H. Varman, N. Bluvshtein, T.N. König, A. Mendelovits, A. Sandler, Applied Clay Science 51 (2011) 43.
[9] V.K. Gupta, J. Suhas, Journal of Environmental Management 90 (2009) 2313.
[10] M. Auta, B.H. Hameed, Chemical Engineering Journal 219 (2012) 198–199.
[11] B. Erdem, A. Özcan, A.S. Özcan, Applied Surface Science 256 (2010) 5422.
[12] A. Olgun, N. Atar, Journal of Industrial and Engineering Chemistry 18 (2012) 1751.
[13] P. Liu, L. Zhang, Separation and Purification Technology 58 (2007) 32.
[14] M. Toifl, D. Nash, F. Roddick, N. Porter, Australian Journal of Soil Research 41 (2003) 1533.
[15] I.A.W. Tan, A.L. Ahmad, B.H. Hameed, Desalination 225 (2008) 13.
[16] D.S. Faust, M.O. Aly, Adsorption processes for water treatment, Butterworth Publishers, 1987, pp. 509.
[17] K.S.W. Sing, D.H. Everett, R.A.W. Haul, L. Moscou, R.A. Pierotti, J. Rouquerol, T. Siemieniewska, Pure and Applied Chemistry 57 (1985) 603.
[18] P. Kumar, R.V. Jasra, T.S.G. Bhat, Industrial & Engineering Chemistry Research 34 (1995) 1440.
[19] J. Temuujin, M. Senna, T. Jadambaa, D. Burmaa, S. Erdenechimeg, K.J.D. MacKenzie, Journal of Chemical Technology & Biotechnology 81 (2006) 688.
[20] F.G.E. Nogueira, J.H. Lopes, A.C. Silva, M. Gonçalves, A.S. Anastácio, K. Sapag, L.C.A. Oliveira, Applied Clay Science 43 (2009) 190.
[21] T.Y. Kim, H.J. Jin, S.S. Park, S.J. Kim, S.Y. Cho, Journal of Industrial and Engineering Chemistry 14 (2008) 714.
[22] E.N. El Qada, S.J. Allen, G.M. Walker, Chemical Engineering Journal 124 (2006) 103.
[23] S. Wang, Z.H. Zhu, Dyes and Pigments 75 (2007) 306.
[24] O. Gök, A.S. Özcan, A. Özcan, Applied Surface Science 256 (2010) 5439.
[25] I. Langmuir, Journal of the American Chemical Society 38 (1916) 2221.
[26] H.M.F. Freundlich, The Journal of Physical Chemistry 57 (1906) 385.
[27] O. Redlich, D.L. Peterson, The Journal of Physical Chemistry 63 (1959) 1024.
[28] Y.S. Ho, W.T. Chiu, C.C. Wang, Bioresource Technology 96 (2005) 1285.
[29] J. Yang, K. Qiu, Chemical Engineering Journal 165 (2010) 209.
[30] A.R. Tehrani-Bagha, H. Nikkar, N.M. Mahmoodi, M. Markazi, F.M. Menger, Desalination 266 (2011) 274.
[31] H. Chen, J. Zhao, A. Zhong, Y. Jin, Chemical Engineering Journal 174 (2011) 143.
[32] C.A.P. Almeida, N.A. Debacher, A.J. Downs, L. Cottet, C.A.D. Mello, Journal of Colloid and Interface Science 332 (2009) 46.
[33] D. Ghosh, K.G. Bhattacharyya, Applied Clay Science 20 (2002) 295.
[34] S. Hong, C. Wen, J. He, F. Gan, Y.S. Ho, Journal of Hazardous Materials 167 (2009) 630.
[35] S. Lagergren, B.K. Svenska, Band 24 (1898) 1.
[36] Y.S. Ho, S. McKay, Process Biochemistry 34 (1999) 451.
[37] M. Anbia, S.A. Hariri, S.N. Ashrafizadeh, Applied Surface Science 256 (2010) 3228.
[38] W.J. Weber, J.C. Morris, Journal of Sanitary Engineering Division, Proceedings of the American Society of Civil Engineers 89 (1963) 30.
[39] Y. Chang, C. Ren, Q. Yang, Z. Zhang, L. Dong, X. Chena, D. Xue, Applied Surface Science 257 (2011) 8610.
[40] T. Santhi, S. Manonmani, T. Smitha, Journal of Hazardous Materials 179 (2010) 178.
[41] T.-Y. Kim, S.-S. Park, S.-Y. Cho, Journal of Industrial and Engineering Chemistry 18 (2012) 1458.
[42] M.J. Jaycock, G.D. Parfitt, Chemistry of Interfaces, Ellis Horwood, Onichester, 1981,
[43] R. Ahmad, R. Kumar, Applied Surface Science 257 (2010) 1628.
[44] M. Auta, B.H. Hameed, Chemical Engineering Journal 171 (2011) 502.
[45] M.A. Martín-Lara, G. Blázquez, A. Ronda, I.L. Rodríguez, M. Calero, Journal of Industrial & Engineering Chemistry 18 (2012) 1006.
[46] N.M. Mahmoodi, B. Hayati, M. Arami, C. Lan, Desalination 268 (2011) 117.
[47] A.A. Ahmad, B.H. Hameed, Journal of Hazardous Materials 175 (2010) 298.
[48] D.C.K. Ko, J.F. Porter, G. McKay, Chemical Engineering Science 55 (2000) 5819.
[49] Y.S. Al-degs, M.A.M. Khraisheh, S.J. Allen, M.N. Ahmad, Journal of Hazardous Materials 165 (2009) 944.
[50] V.C. Taty-costodes, H. Fauduet, C. Porte, Y.S. Ho, Journal of Hazardous Materials 123 (2005) 135.